STM JOURNALS

Journal of
Polymer & Composites

ISSN: 2321-2810 (Online)
ISSN: 2321-8525 (Print)
Volume 14, Special Issue 1, 2026
DOI (Journal): 10.37591/JoPC

https://journals.stmjournals.com/jopc

Research JoPC

Styrene, Carbonate Materials to Minimize Aberration in Free Space Optical Communications

K. Sony[1,*], K. Neeharika[2], C. Santhosh[3]

Abstract

Enhancing wireless connectivity, particularly in harsh weather circumstances, is possible through the use of polymer-based materials in Free Space Optical (FSO) communication systems. In the production of optical components like lenses, beam shapers, and protective enclosures for FSO transmitters and receivers, polymers are being used more and more because of their lightweight, affordable, and adjustable optical qualities. This study examines how well a polymer-integrated FSO link performs over 1–10 km distances when used for high-speed data transmission (up to 10 Gbps) and it is being observed over 5 km range polymer-based fiber is working efficiently than the normal optical fiber .. In Free space optical communications, atmospheric conditions play a pivotal role in deciding the transmission parameters of the communication model and we considered rainfall conditions in different regions and the quality factor using specific attenuation models such as the Carbonneau Model, Japan model, and Suriza model for the rainfall rate in the region of Andhra Pradesh. Efficiency is analyzed in terms of Quality Factor, and it can be seen from the results that both DPSK AND QPSK are suitable for free space communications with a minimum Bit Error Rate , and comparatively, Differential Phase Shift Keying outperforms Quadrature Phase Shift Keying in many ways by using the carbonate material optical fiber.

Keywords: Styrene, **c**arbonate materials, BER, quality factor, attenuation, modulation.

INTRODUCTION

The Free Space link offers a significantly larger optical bandwidth than its RF counterparts, enabling significantly faster data rates. Very narrow laser beams are used in FSO systems. Strong resistance to electromagnetic interference, a high reuse factor, and inherent security. Unlicensed spectrum can be utilized by free space optical link, which can also operate above 300GHz frequency range [1]. Consequently, license fees are not necessary for FSO systems to connect the end user to the existing fiber optic infrastructure, FSO systems were first seen as an effective way to address the "last mile" issue. Significant investments have already been made by telecom providers to increase the capacity of their fiber backbone [2]. This growth in the networks' backbone should be accompanied by a corresponding increase at the network edge, where end users access the system to make the most of the current capacity [3].

Free Space Optics (FSO) is generally utilized in media communications for rapid information transmission over short and significant distances without the requirement for actual links. It assumes a critical part in last-mile networks, giving web access in remote or metropolitan regions where fiber sending is testing. In space

***Author for Correspondence**
K. Sony

[1]Faculty, Department of Electronics and Communication Engineering, Koneru Lakshmaiah Education Foundation, Green Fields, Vaddeswaram, Andhra Pradesh, India
[2]Faculty, Department of Computer Science and Engineering, Andhra Loyola Institute of Engineering and Technology, Vijayawada, Andhra Pradesh, India
[3]Faculty, Department of Electronics and Communication Engineering, Koneru Lakshmaiah Education Foundation, Green Fields, Vaddeswaram, Andhra Pradesh, India

Received Date: November 18, 2025
Accepted Date: December 01, 2025
Published Date: January 07, 2026

Citation: K. Sony, K. Neeharika, C. Santhosh. Styrene, Carbonate Materials to Minimize Aberration in Free Space Optical Communications. Journal of Polymer & Composites. 2026; 14(Special Issue 1): S675–S686p.

correspondence, FSO empowers rapid information joins between satellites, ground stations, and interplanetary missions, offering effective and solid correspondence [4].

The primary determinant of a material's use in lens design is its optical characteristics. Excellent transmission in the visible (VIS) and near-infrared (NIR) spectrums The thickness of the film and the composition of the material affect transmittance. Between 500 and 1600 nm, thin films (~100 µm) showed roughly 90% transmission. At 1660–1700 nm, weak absorption bands were visible, and transmission decreased after 2200 nm. Transmittance varied from 75 to 85% for various polymers in the VIS region.. Additionally, the critical angle approach was used to determine the refractive index precisely.[5].

However, Conversely, an FSO is susceptible to unfavorable atmospheric conditions. In other words, a sole beam FSO is susceptible to weather conditions that attenuate light sources, such as rain, haze, dust, drizzle, fog, smog, and weather instability [6].

Polystyrene will introduce less chromatic focal shift per unit thickness than polycarbonate for broadband optical signals (such as white light beacon or broad-spectrum detection) because of its higher Abbe number (~57), which results in lesser dispersion.

The suggested algorithm uses a free-space wireless optical link as the communication channel and consists of various input parameters like the continuous wave laser and pseudo-random generator, avalanche photodetectors, and Bit error rate analyzer for performance evaluation are all included in the optical receiver's design [7]. A highly sensitive APD detector is the best option for picking weak signals [8]. An electrical data signal is transformed into an optical signal using an optical transmitter. It consists of a photon source, like a laser or LED, and, crucially, (PRBS) all of which are necessary for the optical signal to be transmitted. Stimulation emission in Lasers makes this coherent light possible. The achievable optical power for transmission purposes is directly influenced by the wavelength of the laser. When modulated, (CW) laser produces light at high frequencies for frequency-domain measurements [9]. These days, CW lasers are widely used in many industries, such as aerospace, material processing, and military applications.

Avalanche Photo Diode (APD) is used as the detector in FSO Systems, where the FSO Link is implemented with the help of Phase shift keying (PSK) and different types, such as differential phase shift (DPSK) and quadrature phase shift (QPSK) PSK transmits information via the optical signal's phase, but it necessitates coherent detection, which raises the complexity and expense of the system [10].

Reduce Fresnel losses and surface scattering by applying hard coats and anti-reflection (AR) coatings. Additionally, this preserves wavefront quality by shielding polymers, which are more prone to scratches.

In contrast, DPSK uses the phase difference between successive bits to encode information, which makes it ideal for underwater settings. By either maintaining the same data rate as binary PSK (BPSK) while requiring less bandwidth or by doubling the data rate of BPSK without increasing bandwidth, QPSK provides flexibility [11]. By varying the range and attenuation values, FSO channels can be simulated. Bit error rate (BER) and Q-factor measurements, represented by eye diagrams, are used to assess the performance of these FSO systems. This evaluation offers information on the system's effectiveness, likelihood of noise, and general dependability. Careful modification of communication parameters guarantees a precise and safe configuration [12].

DPSK is a widely used phase modulation technique in which the carrier signal's phase is altered to represent data. This scheme enables the effective encoding of binary data since each phase shift of the

ISSN: 2321-2810 (Online), ISSN: 2321-8525 (Print)

modulated signal is dependent on the phase of the preceding element. High-speed optical networks frequently use DPSK for packet routing [13].. As a result, under ideal circumstances, QPSK can double the data rate when compared to standard PSK for the same bandwidth, increasing bandwidth efficiency by a factor of two [14]. The channel used is free space, and it is prone to severe adverse atmospheric conditions. When the optical signal interacts with the rain droplets, the signal will get attenuated [15]. Different rain-specific attenuation models are available, which will estimate the attenuation depending on the rainfall rate and the size of the rain droplet the attenuation will change [16].

Manufacturing wavefront error and thermooptic effects:

Polycarbonate has a higher mechanical toughness and a temperature-dependent refractive index (datasheets show that nD varies with temperature); aberration is caused by both thermal gradients and molding stress, which also result in index/non-uniformity and form error. Choose low-CTE optical grades, anneal, or manage molding stress. Divergence and beam spread can be obtained by using the following equations

$$w(z) = w_0\sqrt{1 + \left(\frac{\lambda z}{\pi w_0^2 n(\lambda)}\right)^2} \tag{1}$$

$$\theta(\lambda) \approx \frac{\lambda}{\pi w_0 n(\lambda)} \tag{2}$$

w_0= waist, z= propagation distance, $n(\lambda)$= refractive index.

Scattering loss

$$\alpha_{\text{scat}}(\lambda) \propto \frac{1}{\lambda^4} \tag{2}$$

For low aberration/scatter, polymer optics must meet surface-figure and surface-roughness specifications similar to those of glass; polymer surfaces are more prone to scratches; take into account hard coats and AR coatings.

Link margin and Q-factor

Optical SNR

$$\text{SNR}_{\text{opt}} \approx \frac{R\,P_r}{h\nu B} \tag{3}$$

Q-factor

$$Q \approx \sqrt{2\ \text{SNR}_{\text{opt}}} = \sqrt{\frac{2R\,P_r}{h\nu B}} \tag{4}$$

SIMULATION SETUP

The Simulation setup is illustrated in Figures 1 and 2, where DPSK and QPSK Modulations are used to estimate the quality factor and BER. The parameters used to simulate FSO modulation are listed in Table 1. Atmospheric conditions play a crucial role in estimating the attenuation [17]. Rainfall attenuation has a major effect on signal quality in free-space optical (FSO) communication because it can significantly scatter and absorb optical signals. Models such as Japan, Suriza, and Carbonneau models are frequently used to forecast and control these effects [18]. The design and optimization of FSO systems under varied weather conditions are supported by these models, which offer a means of connecting rainfall rate to signal attenuation [19]. Heavy seasonal rains and monsoon seasons are two examples of local climate factors that affect rainfall patterns and the attenuation that goes along with them [20]. The rainfall intensity, which is commonly expressed in millimeters per hour (mm/h), is used in this model to define the attenuation brought on by rain [21].

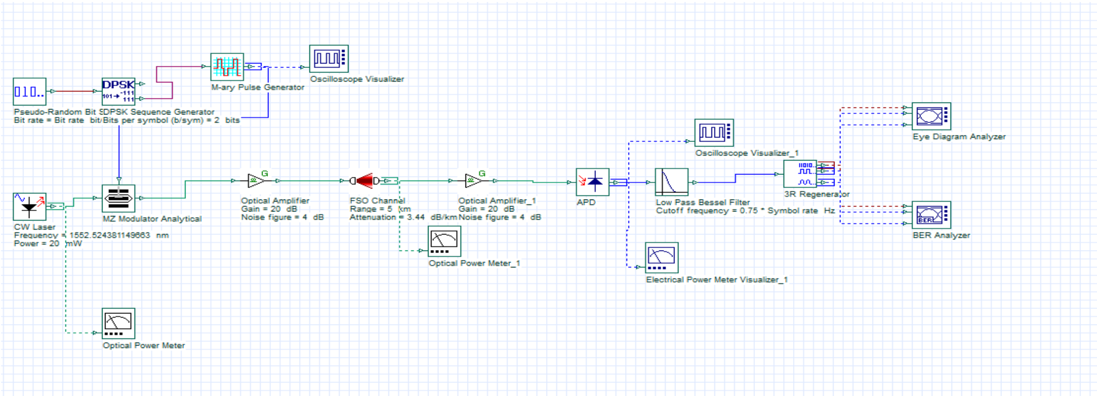

Figure 1. System layout for DPSK modulation.

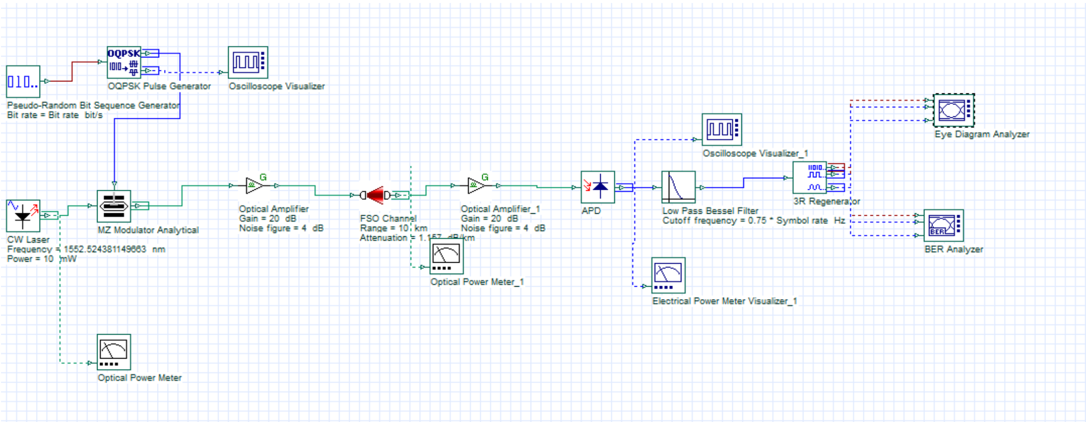

Figure 2. System layout for QPSK modulation.

Table 1. Parameter required to design the FSO Link

Parameters	**Value**
Modulation Schemes	DPSK &QPSK
Distance (Km)	10-Jan
Wavelength	1550nm
Transmitted Power	10mW
Attenuation	0-5 dB/Km
Transmitter Aperture	2.5cm
Amplifier Gain	20 dB

The Rainfall rate is 3.44 mm/hr.in the region of Vaddeswaram, AP, which is collected from KL Weather Station, and data is verified from the AP Meteorological Department website. The attenuation is calculated using the specific attenuation equation as follows [22]:

$$A = k \cdot R^{\alpha} \tag{5}$$

Where A is the rain attenuation, R is the Rainfall Rate
k, α are the coefficient values

A powerful electric field that promotes carrier multiplication allows an avalanche photodiode (APD), a highly sensitive photo detector [23]. Even though the conversion is intrinsically nonlinear, this feature makes APDs efficient at transforming optical signals into electrical ones [24]. APDs have a nonlinear response that is influenced by temperature and supply voltage because the multiplication factor changes with these variables [25].

We integrate well-known statistical turbulence models into the link simulation to generate more accurate Q-factor and BER estimations for outdoor or long-range links (and to reflect the main effects in tropical regions). In particular, we use (i) the log-normal distribution for light turbulence, (ii) the Gamma–Gamma distribution for moderate-to-strong turbulence, and (iii) Rytov-variance expressions to identify the turbulence regime in order to represent irradiance variations I. The irradiance distribution is used to average the instantaneous BER under fading:

where $\gamma(I)$is the instantaneous electrical SNR as a function of irradiance and $f_I(I)$is the chosen irradiance PDF.

In our simulations we use the following model forms. For log-normal fading (weak turbulence), if $X = \ln\ I \sim \mathcal{N}(\mu_X, \sigma_X^2)$,

$$f_I(I) = \frac{1}{I\sqrt{2\pi}\,\sigma_X} \exp\ \left(-\frac{(\ln\ I-\mu_X)^2}{2\sigma_X^2}\right), \tag{6}$$

with scintillation index $\sigma_I^2 = \exp\,(\sigma_X^2) - 1$.

For moderate-to-strong turbulence the Gamma–Gamma PDF is used:

$$f_I(I) = \frac{2(\alpha\beta)^{\frac{\alpha+\beta}{2}}}{\Gamma(\alpha)\Gamma(\beta)}\, I^{\frac{\alpha+\beta}{2}-1}\, K_{\alpha-\beta}\,(2\sqrt{\alpha\beta I}\,), \tag{7}$$

where $\alpha, \beta$are turbulence parameters

In Table 2, different specific rain attenuation models are listed, and using the same attenuation for the specified optical link is estimated, and the resulting attenuation is listed in Table 3.

Transmitted till 6 Km and using the suriza model at the attenuation of 1.157 dB/Km without any errors, the data is sent successfully till 10km. From the statistics for DPSK modulation, the suriza model works best up to 10kms with a good quality factor [28].

Figures 3 (a) (b) and (c) display the eye diagram for the three models, and based on eye height suriza model can be used for transmission [29].

Table 2. Specific rain attenuation values.

Model type	**Coefficient value**
Carbonneau Model	1.076,0.67
Japan Model	1.58,0.63
uriza Model	0.4195,0.8486

Table 3. Performance parameters of DPSK modulation.

Distance (Km)	**Japan Model Attenuation 3.44 dB/Km**		**Carbonnean Model Attenuation 2.46 dB/Km**		**Suriza Model Attenuation 1.157 dB/Km**	
	Quality Factor(Q)	**Bit Error Rate**	**Quality Factor (Q)**	**Bit Error Rate**	**Quality Factor (Q)**	**Bit Error Rate**
1	694	0	707	0	871	0
2	279	0	349	0	488	0
3	132	0	183	0	272	0
4	66	0	102	0	196	0
5	34.62	3.32081×10^{-146}	63	0	138	0
7	0	1	24.81	2.11227×10^{-136}	103	0
10	0	1	0	1	33	3.320×10^{-242}

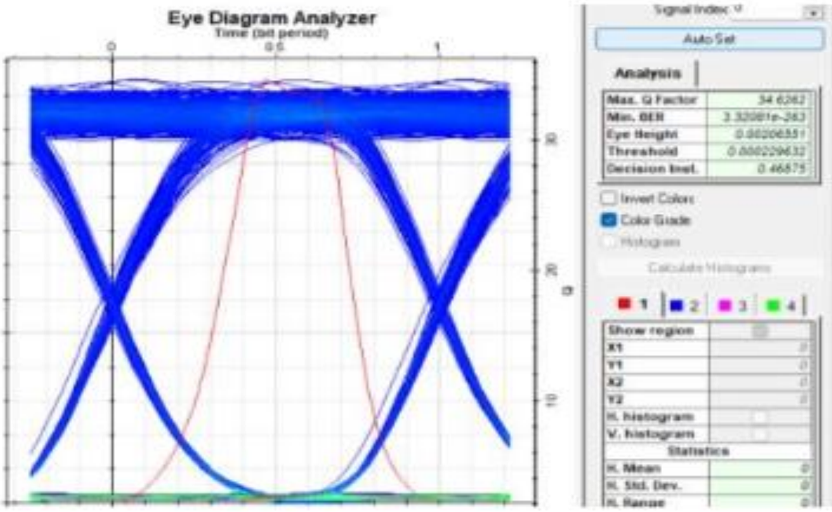

Figure 3. (a) DPSK Eye pattern using using Japan model at 5Km.

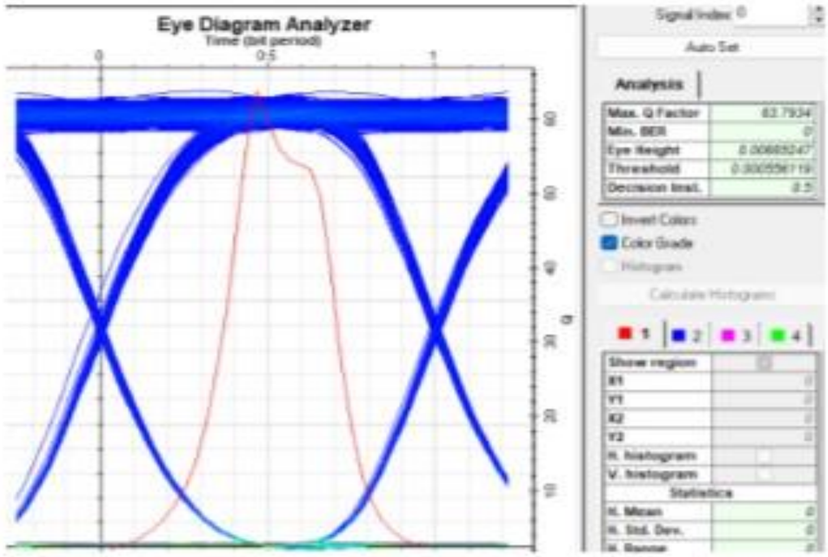

Figure 3. (b) DPSK Eye pattern using Carbonnean Model at 5Km.

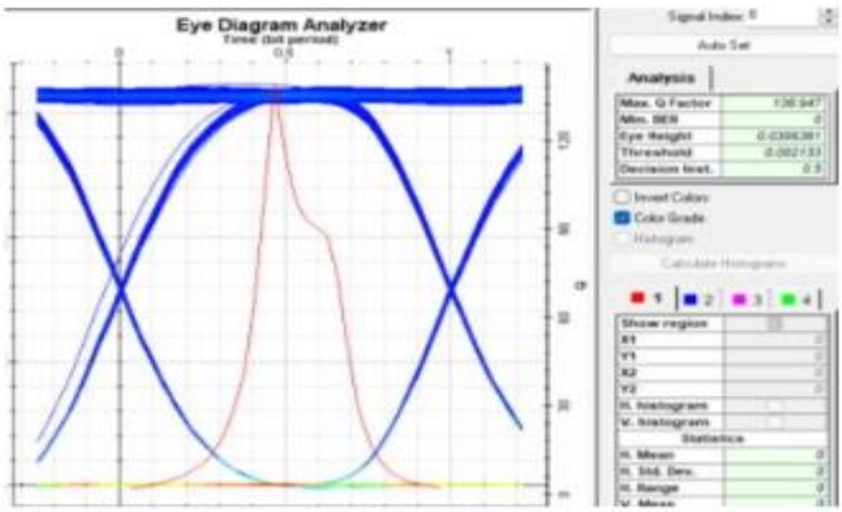

Figure 3. (c) DPSK Eye pattern Suriza Model at 5Km.

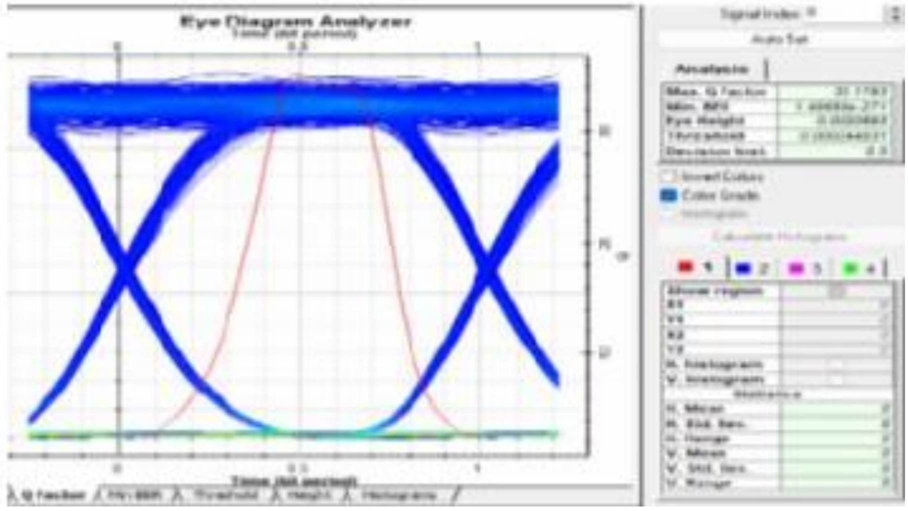

Figure 4. (a) OPSK Eye pattern using using Japan model at 5Km.

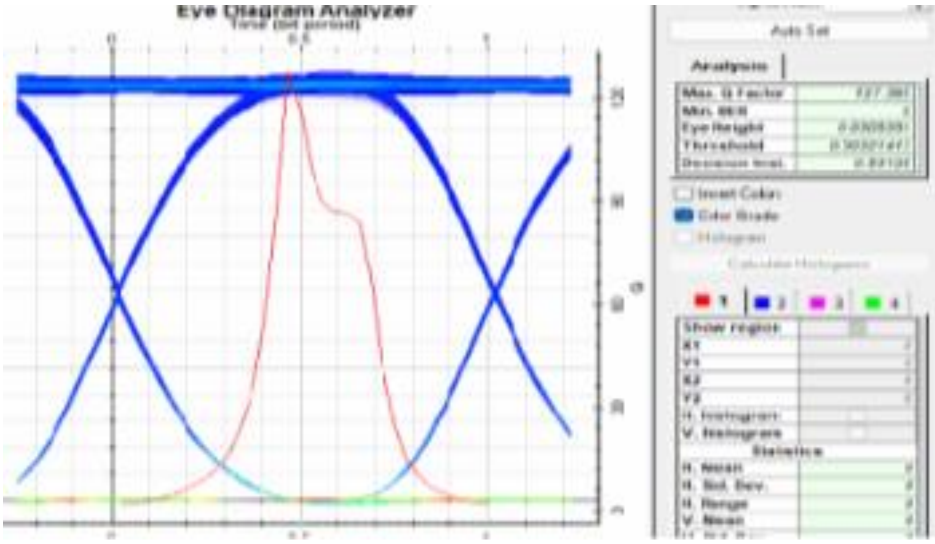

Figure 4. (b) OPSK Eye pattern using Carbonnean Model at 5Km.

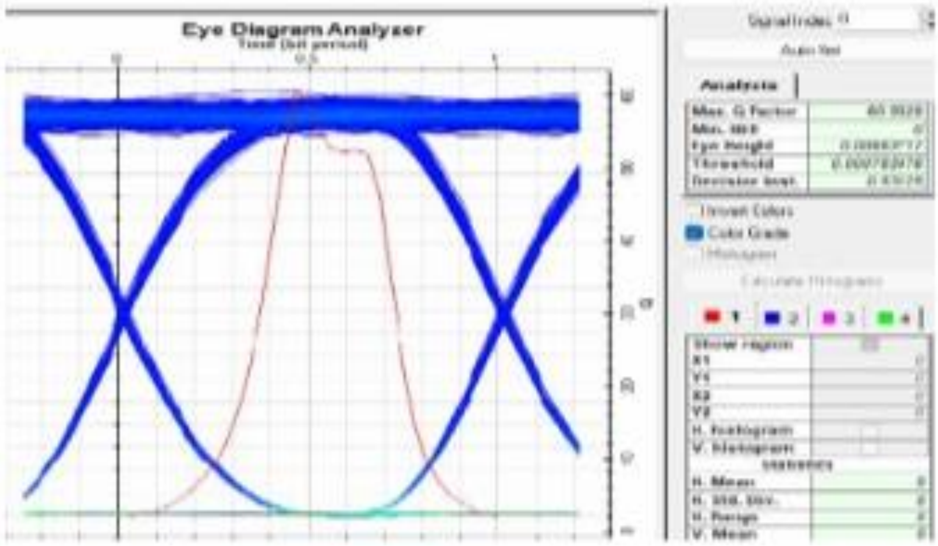

Figure 4. (c) OPSK Eye pattern Suriza Model at 5Km.

Using QPSK, the Modulation Quality factor and BER are analyzed [30]. When the distance increases, the quality factor, and the bit error rate are reduced for the Japan model at the attenuation of 3.44 dB/Km at a distance of 1 Km, the Q Factor is 476, and when the distance is increased to 4 Km, the quality factors are 243,123,65 listed in Table 4 [31–32].

The message can be successfully transmitted only till 6 Km, and using the suriza model at the attenuation of 1.157 dB/Km without any errors, the data is sent successfully till 10km. Figure 4. (a) (b) (c) displays the eye diagram for the three models based on eye height [33].

The quality factors for each design, however, converge as the distance increases to 8–10 km, suggesting comparable performance over longer distances [34]. Although Suriza exhibits a slight advantage at closer ranges, the research indicates that signal quality in DPSK systems is more noticeable, and as the distance gets closer to 10 km, it gradually levels off. [35] Suriza retains somewhat higher quality factors than

Carbonnean and Japan among the configurations in the early range, but the differences become less noticeable as the distance passes 8 km, at which point all configurations perform similarly [36]. Drastically deteriorates with increasing transmission distance. In Figure 5, Figure 6, and Figure 7, as the distance grows, the quality factor decreases in all three setups [37]. Suriza performs slightly better at shorter ranges, which is consistent with the usual signal loss in OQPSK systems over longer distances [38].

Table 4. Performance parameters of OQPSK modulation.

Distance (Km)	Japan Model Attenuation 3.44 dB/Km		Carbonnean Model Attenuation 2.46 dB/Km		Suriza Model Attenuation 1.157 dB/Km	
	Quality Factor (Q)	*Bit Error Rate*	*Quality Factor (Q)*	*Bit Error Rate*	*Quality Factor (Q)*	*Bit Error Rate*
1	476	0	481	0	521	0
2	243	0	294	0	356	0
3	123	0	166	0	239	0
4	65	0	102	0	178	0
5	35	1.496×10^{-271}	60	0	127	0
7	0	1	37	8.35227×10^{-314}	74	0
10	0	1	15	0	33	1.52×10^{-24}

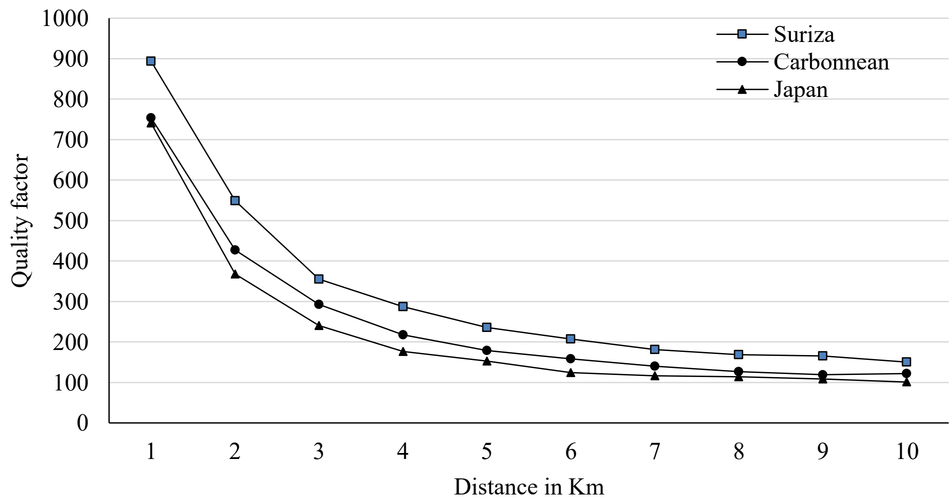

Figure 5. Distance vs. quality factor for DPSK modulation.

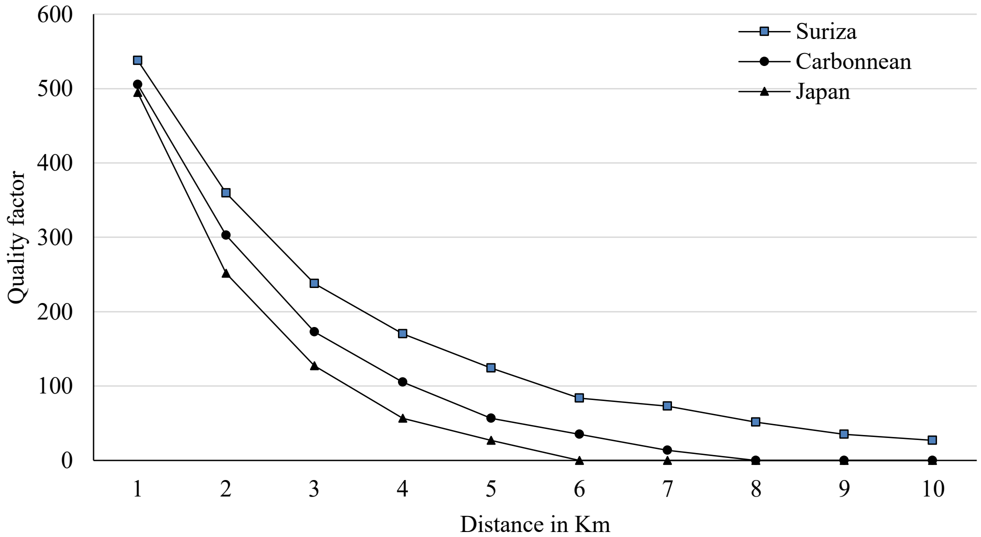

Figure 6. Distance vs. quality factor for OQPSK modulation.

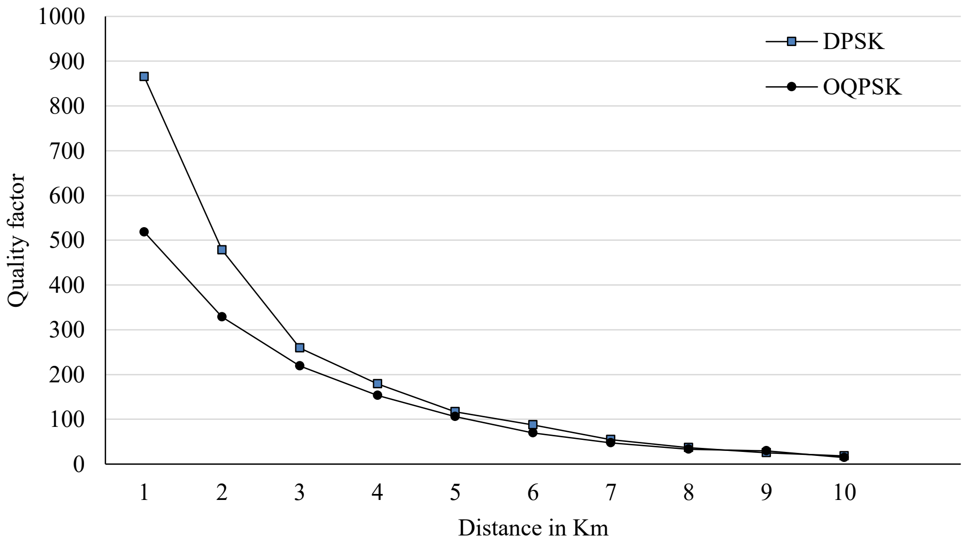

Figure 7. Comparison of DPSK & OQPSK modulation.

CONCLUSION

Very high transmission speeds, wide bandwidth, low latency, and enhanced data rates in free-space optical communication networks are becoming more and more necessary because of the integration of 5G technology and the increase in human activity. Over a range of distances (1–10 km), the quality factor of OQPSK and DPSK is compared in comparison to OQPSK, DPSK has a greater quality factor, especially over shorter distances (1–3 km). But as the distance grows, the quality factor for both systems falls. The performance of the two approaches starts to converge at 4 km, and a similar pattern is seen up to 10 km, where the quality factors are almost identical. In this study, DPSK and QPSK modulation methods are used for free-space optical communication, while APDs are used for photodetection.

The results show that distortion rises with distance and that Suriza in DPSK achieves a satisfactory Q factor and eye diagram at 10 km. With the use of simulation analysis utilizing Opti System software, this comparison study is carried out for several rain attenuation model types by varying the attenuation parameters in an optical wireless channel With the use of simulation analysis utilizing

Opti System software; this comparison study is carried out for several rain attenuation model types by varying the attenuation parameters in an optical wireless channel. According to the results of the study, the DPSK modulation type has a significantly higher Q-factor than QPSK. When compared to the recently employed modulation techniques, both modulation schemes are successful in free-space optical communication systems since they have nearly identical performance parameters in the same environment.

REFERENCES

1. Wang, Q. Liu, W. Lu, High-speed visible light communications: enabling technologies and state of the art. Appl. Sci. 8(4), 589 (2018). https://doi.org/10.3390/app8040589
2. Colella, P.R. Woodward, The piecewise parabolic method (PPM) for gas-dynamical simulations. J. Comput. Phys. 54(1), 174–201 (1984). https://doi.org/10.1016/0021-9991(84)90143-8
3. Shafi F, Kumar A, Nakkeeran R. Performance analysis of free space optical networks under external limiting factors. Results in Optics. 2024 Feb 1;14:100615.
4. Alkholidi, K.S. Altowij, Free space optical communications—theory and practices. Contemp. Issues Wirel. Commun. (2014). https://doi.org/10.5772/58884
5. Sadiq, M.A. Kabir, Design and implementation of recon- figurable ASK and FSK modulation and demodulation algorithm on FPGA (Field Programmable Gate Array). Sens. Int. 3, 100155 (2022). https://doi.org/10.1016/j.sintl.2021.100155
6. Hilal A. Fadhil, Angela Amphawan, Hasrul A.B. Shamsuddin, Thanaa Hussein Abd, Hamza M.R. Al-Khafaji, S.A. Aljunid, Nasim Ahmed, Optimization of free space optics parameters: An optimum solution for bad weather conditions, Optik, Volume 124, Issue 19, 2013, Pages 3969–3973, ISSN 0030-4026,https://doi.org/10.1016/j.ijleo.2012.11.059.
7. Zhu, M. Funabashi, Z. Pan, L. Paraschis, D.L. Harris, S.B. Yoo, High-performance optical 3R regeneration for scalable fiber transmission system applications. J. Lightwave Technol. 25(2), 504–511 (2007). https://doi.org/10.1109/JLT.2006.888256
8. Tung, M. Zhang, C.-T. Lin, K. Kurabayashi, S.J. Sker- los, PDMS-based optofluidic micro flow cytometer with two-color, multi-angle fluorescence detection capability using PIN photodiodes. Sens. Actuators, B Chem. 98(2–3), 356–367 (2004). https://doi.org/10.1016/j.snb.2003.10.010
9. Rashidi, Z. and Majidi, M. (2024). Energy and Throughput Management in Wireless Body Area Network with Wireless Information and Energy Transfer using Reinforcement Learning. *International Journal of Engineering*, *37*(11), 2314-2324. https:// doi: 10.5829/ije.2024.37.11b.16
10. Sony, Babu K. Rajesh, Ch. Suneetha, N. Venkatesh, and Y. Dasaratha Rami Reddy (2023), Modelling System Parameters for Improvised Performance in Free Space Optics (FSO) Networks. IJEER 11(ngwcn), 10-14. DOI: 10.37391/ijeer.11ngwcn02.
11. Kaur J., Kaur B., Singh K.Design and Performance Investigation of Intersatellite Optical Wireless Communication System Employing Modulation Techniques (2017) Wireless Personal Communications, 94 (3), pp. 793 - 807, Cited 8 times. DOI: 10.1007/s11277-016-3651-8
12. Rashidi, Z. and Majidi, M. (2024). Energy and Throughput Management in Wireless Body Area Network with Wireless Information and Energy Transfer using Reinforcement Learning. *International Journal of Engineering*, *37*(11), 2314–2324. doi: 10.5829/ije.2024.37.11b.16
13. Ghassemlooy, A. Hayes, N.L. Seed, E. Kaluarachchi, Digital pulse interval modulation for optical communications. IEEE Commun. Mag. 36(12), 95–99 (1998). https://doi.org/10.1109/35.735885
14. Babu T, Jayalakshmi V. Conglomerate energy efficient Elgamal encryption-based data aggregation cryptosystems in Wireless Sensor Network. International Journal of Engineering, Transactions B: Applications. 2022;35(2):417–24. 10.5829/IJE.2022.35.02B.18
15. Madhu Krishna, K. and Naveen Kumar, P. (2023). Improving the Position Accuracy of Rover Receiver using Differential Positioning in Indian Regional Navigation Satellite System. *International Journal of Engineering*, *36*(3), 497–504. Doi: 10.5829/ije.2023.36.03c.09
16. Sachdeva S., Kaur S., Arora R., Sindhwani M., Arora K., Cho W., Joshi G.P., Doo I.C.Ultra-High Capacity Optical Satellite Communication System Using PDM-256-QAM and Optical Angular Momentum Beams(2023) Sensors, 23 (2), art. no. 786, Cited 10 times. DOI: 10.3390/s23020786

17. Manda, R. and Gowri, R. (2022). Universal Filtered Multicarrier Receiver Complexity Reduction to Orthogonal Frequency Division Multiplexing Receiver. *International Journal of Engineering*, *35*(4), 725–731. doi: 10.5829/ije.2022.35.04A.12
18. Malik, P. Singh, Free space optics: current applications and future challenges. Int. J. Opt. (2015). https://doi.org/10.1155/ 2015/945483
19. Seyed Aghaei, S. M. H., Rashno, A. and Fadaei, S. (2025). Classification of Optical Coherence Tomography Images Using Generative Adversarial Networks. International Journal of Engineering, 38(2), 389–399. doi: 10.5829/ije.2025.38.02b.13
20. Wu, S. He, Y. Ren, N. Wang, S.C.M. Ho, G. Song, Design of a new stress wave-based pulse position modulation (PPM) communication system with piezoceramic transducers. Sensors 19(3), 558 (2019). https://doi.org/10.3390/s19030558
21. Muhammad, M. Aly Mohamed, H.A. Fayed, R.A. AbdelRassou, Adaptive free space optic system based on visibility detector to overcome atmospheric attenuation. Results Phys. 14, 102392 (2019). https://doi.org/10.1016/j.rinp.2019.102392
22. Eremin, Scattering | Scattering Theory in Encyclopedia of Modern Optics, 326–330 (2005). https://doi.org/10.1016/B0-12- 369395-0/00682-5
23. Ojo, J.S., Ojo, O.L., Olaitan, J.A. Characterization and spatial distributions of atmospheric visibility, relative humidity and temperature for the possible effect on optical communication links in Nigeria (2024) Journal of Optics (India), 53 (1), pp. 416-427. DOI: 10.1007/s12596-023-01211-z
24. Firdaus, F., Fadhillah, I. Ahmad, N. A. and Mohd Alic, A. A. (2023). A Light Solution for Device Diversity Problem in a Wireless Local Area Network Fingerprint Indoor Positioning System. *International Journal of Engineering*, *36*(4), 649–658. doi: 10.5829/ije.2023.36.04a.05
25. De, A., Adhikari, A., Maitra, A. Prerain Scintillations of Ku-Band Satellite Signal about Cloud and Convective Parameters at a Tropical Location (2017) IEEE Geoscience and Remote Sensing Letters, 14 (2), art. no. 7805270, pp. 252–256. doi: 10.1109/LGRS.2016.2637441
26. Jain, R. Bahl, A. Banik, Demonstration of RZ-OOK modulation scheme for high-speed optical data transmission, in 2014 11th International Conference on Wireless and Optical Communications Networks (WOCN) (IEEE, 2014), pp. 1–5. https://doi.org/ 10.1109/WOCN.2014.6923082
27. Zhu, M. Funabashi, Z. Pan, L. Paraschis, D.L. Harris, S.B. Yoo, High-performance optical 3R regeneration for scalable fiber transmission system applications. J. Lightwave Technol. 25(2), 504–511 (2007). https://doi.org/10.1109/JLT.2006.888256
28. Ghassemlooy, A. Hayes, N.L. Seed, E. Kaluarachchi, Digital pulse interval modulation for optical communications. IEEE Commun. Mag. 36(12), 95–99 (1998). https://doi.org/10.1109/35. 735885
29. Sharma V., Kumar N.Modeling of 2.5 Gbps-inter-satellite link (ISL) in satellite optical wireless communication (IsOWC) system (2013) Optik, 124 (23), pp. 6182–6185, Cited 17 times. DOI: 10.1016/j.ijleo.2013.04.094
30. Balamurugan, V., Vedanarayanan, V., Sahaya Anselin Nisha, A, Narmadha, R. and Amirthalakshmi, T. M. (2022). Multi-label Text Categorization using Error-correcting Output Coding with Weighted Probability. *International Journal of Engineering*, *35*(8), 1516-1523. doi: 10.5829/ije.2022.35.08b.08
31. Howldar, S. , Balaji, B. and Srinivasa Rao, K. (2023). Design and Analysis of Hetero Dielectric Dual Material Gate Underlap Spacer Tunnel Field Effect Transistor. International Journal of Engineering, 36(12), 2137–2144. doi: 10.5829/ije.2023.36.12c.01
32. Howldar, S. , Balaji, B. and Srinivasa Rao, K. (2023). Design and Qualitative Analysis of Hetero Dielectric Tunnel Field Effect Transistor Device. International Journal of Engineering, 36(6), 1129–1135. doi:10.5829/ije.2023.36.06c.11
33. Gowthami, Y. , Balaji, B. and Srinivasa Rao, K. (2023). Performance Analysis and Optimization of Asymmetric Front and Back Pi Gates with Dual Material in Gallium Nitride High Electron Mobility Transistor for Nano Electronics Application. International Journal of Engineering, 36(7), 1269–1277. doi: 10.5829/ije.2023.36.07a.08

34. Radhamma, E. , Vemana Chary, D. , Krishnamurthy, A. , Venkatarami Reddy, D. , Sreenivasa Rao, D. , Gowthami, Y. and Balaji, B. (2023). Performance Analysis of High-K Dielectric Heterojunction High Electron Mobility Transistor for RF Applications. International Journal of Engineering, 36(9), 1652–1658. doi: 10.5829/ije.2023.36.09c.09
35. Krishnamurthy, A. , Venkatarami Reddy, D. , Radhamma, E. , Jyothirmayee, B. , Sreenivasa Rao, D. , Agarwal, V. and Balaji, B. (2023). Design and Performance Analysis of 6H-SiC Metal-Semiconductor Field-Effect Transistor with Undoped and Recessed Area under Gate in 10nm Technology. International Journal of Engineering, 36(12), 2264-2271. doi: 10.5829/ije.2023.36.12c.16
36. Howldar, S. , Balaji, B. and Srinivasa Rao, K. (2024). Gate Oxide Thickness and Drain Current Variation of Dual Gate Tunnel Field Effect Transistor. International Journal of Engineering, 37(3), 520–528. doi: 10.5829/ije.2024.37.03c.09
37. Rohith Sai, K. , Girija Sravani, K. , Srinivasa Rao, K. , Balaji, B. and Agarwal, V. (2024). Design and Performance Analysis of High-k Gate All Around Fin-field Effect Transistor. International Journal of Engineering, 37(3), 476–483. doi: 10.5829/ije.2024.37.03c.04
38. Howldar, S. , Balaji, B. and Srinivasa Rao, K. (2024). Investigation and Analysis of Dual Metal Gate Overlap on Drain Side Tunneling Field Effect Transistor with Spacer in 10nm Node. International Journal of Engineering, 37(5), 887–895. doi: 10.5829/ije.2024.37.05b.07.

